

Genomic architecture controls multivariate adaptation to climate change

Drew E. Terasaki Hart^{a,b,c,1} and Ian J. Wang^a

^aDepartment of Environmental Science, Policy, and Management, University of California, Berkeley, CA 94720, USA; ^bThe Nature Conservancy, Arlington, VA 22203, USA; ^cCSIRO Environment, Brisbane, Queensland 4102, Australia

This manuscript was compiled on December 11, 2023

1 **As climate change advances, environmental gradients may decouple, generating novel multivariate environments that stress wild populations.**
2 **A commonly invoked mechanism of evolutionary rescue is adaptive gene flow tracking climate shifts, but gene flow from populations**
3 **inhabiting similar conditions on one environmental axis could cause maladaptive introgression when populations are adapted to different**
4 **environmental variables that do not shift together. Genomic architecture can play an important role in determining the effectiveness and relative**
5 **magnitudes of adaptive gene flow and *in situ* adaptation. This may have direct consequences for how species respond to climate change**
6 **but is often overlooked. Here, we simulated microevolutionary responses to environmental change under scenarios defined by variation in**
7 **the polygenicity, linkage, and genetic redundancy of two independent traits, one of which is adapted to a gradient that shifts under climate**
8 **change. We used these simulations to examine how genomic architecture influences evolutionary outcomes under climate change. We found**
9 **that climate-tracking (up-gradient) gene flow, though present in all scenarios, was strongly constrained under scenarios of lower linkage**
10 **and higher polygenicity and redundancy, suggesting *in situ* adaptation as the predominant mechanism of evolutionary rescue under these**
11 **conditions. We also found that high polygenicity caused increased maladaptation and demographic decline, a concerning result given that**
12 **many climate-adapted traits may be polygenic. Finally, in scenarios with high redundancy we observed increased adaptive capacity. This**
13 **finding adds to the growing recognition of the importance of redundancy in mediating *in situ* adaptive capacity and suggests opportunities for**
14 **better understanding the climatic vulnerability of real populations.**

adaptation | climate change | landscape genomics | spatial simulation | gene flow | genomic architecture | genetic redundancy

1 Climate change is one of the foremost threats to biodi-
2 versity in the Anthropocene. The ability of species to
3 persist within their current ranges will likely depend largely
4 upon their abilities to locally adapt to new climate conditions
5 — a concept frequently referred to as ‘adaptive capacity’ or
6 ‘evolutionary potential’ (1–5). Because beneficial *de novo*
7 mutations take a long time to arise, this adaptation will likely
8 be facilitated by the reconfiguration of existing adaptive ge-
9 netic diversity (6). A common conceptual model underlying
10 this scenario is that of adaptive gene flow tracking a shifting
11 climatic gradient (7, 8), which would bring beneficial genes
12 into recipient populations from ‘climate-suitable’ populations
13 whose current climates approximate future local conditions (9).
14 This model of adaptive gene flow has both theoretical (10–12)
15 and empirical (13, 14) support but meets resistance under
16 conditions in which gene flow can be maladaptive (11, 15–19).
17 In these circumstances, shifting allelic covariance — the *in situ*
18 recombination of standing genetic variation into new, adaptive
19 genotypes — could be a more efficient mechanism underlying
20 local adaptation to environmental change.

21 In recent decades, research bridging the fields of molecu-
22 lar population genetics and quantitative genetics (20–23) has
23 revealed that the genomic architecture of a trait is a core
24 determinant of whether and how that trait becomes locally
25 adapted (24). Among the key aspects of genomic architec-
26 ture that influence adaptation (21, 24–26) are the number of
27 loci underlying a trait (henceforth, ‘polygenicity’), the rate
28 of recombination between these loci (i.e., linkage), and the
29 number of distinct genotypes that yield identical phenotypes
30 (henceforth, ‘genotypic redundancy’). Previous research sug-
31 gests that ecologically-important traits can vary from having

32 few loci of large effect (27, 28) to many loci of small effect
33 (20, 29–32) and shows that variation in polygenicity can de-
34 termine the rate and nature of local adaptation (33). Linkage
35 controls the likelihood that adaptive alleles cluster together,
36 essentially forming alleles of larger effect size that are stronger
37 targets of selection and more resistant to swamping gene flow
38 (25), thereby facilitating local adaptation (12). Genotypic
39 redundancy — a form of genetic redundancy that is defined
40 as when more than one genotype can produce the same phe-
41 notype (34) — can facilitate local adaptation by allowing the
42 existence of a stable phenotypic cline governed by concerted
43 shifts in underlying allele frequencies (33, 35, 36). We refer to
44 this phenomenon as ‘transient genomic architecture.’

45 The influence of genomic architecture on the nature and
46 outcomes of local adaptation to changing environmental gradi-
47 ents has been studied to a limited extent, with nearly exclusive
48 focus on univariate models of the selective environment (but
49 see (37)). These models have limitations for studying adap-
50 tation to climate change because, in nature, species can be
51 adapted to multiple, independent environmental gradients
52 (38) that can shift differentially, and thus decouple, as climate
53 change advances (39, 40), leading to the emergence of novel
54 multivariate landscapes (41–43). Thus, it is important to in-
55 vestigate how the genomic architectures of multiple traits can
56 combine to drive multivariate adaptation under climate change.
57 Gene flow from ‘climate-suitable’ portions of a species’ range
58 is often assumed to be beneficial for adaptation to climate
59 change. This may be accurate from the perspective of a single
60 trait adapted to a shifting climatic gradient, but it may be an
61 invalid assumption if the gene flow also carries linked variation
62 for a trait adapted to a second environmental variable from

component	level	parameter value
genotypic redundancy	low:	redund = 1
	high:	redund = 2
polygenicity	low:	$n_loci = 4 \times redund$
	mod:	$n_loci = 20 \times redund$
	high:	$n_loci = 100 \times redund$
linkage	low:	recomb = 0.5
	mod:	recomb = 0.05
	high:	recomb = 0.005

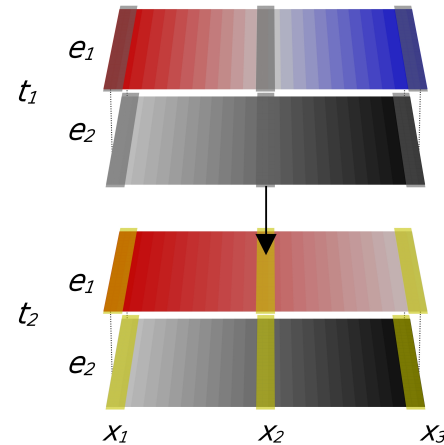
Table 1. Parameter values used for each of the three focal components of genomic architecture. The full factorial combinations of these parameter values constitute the set of 18 simulation scenarios for which we present results.

63 which the shifting gradient has decoupled. Under this scenario,
 64 gene flow may introduce alleles for the second trait that are dis-
 65 advantageous and that could counteract any fitness advantage
 66 gained through the first trait. Thus, the genomic architectures
 67 of both traits may determine evolutionary outcomes by con-
 68 trolling the relative likelihoods of adaptation by gene flow and
 69 of *in situ* adaptation by shifting allelic covariance (10, 37).

70 Spatially-explicit simulation is one of our strongest tools
 71 for improving our understanding of the complex dynamics of
 72 gene flow and adaptation under climate change (44). In this
 73 study, we use individual-based, spatially-explicit simulations,
 74 constructed in Geonomics (45), to test how genomic architec-
 75 ture influences multivariate adaptation to climate change. We
 76 simulate the adaptation of a single population continuously
 77 distributed on a two-dimensional landscape composed of two
 78 environmental variables, each structured as a gradient that
 79 runs parallel to the x-axis (Fig. 1) and that exerts selection
 80 on a separate trait. In our main models, we then simulate
 81 climate change on that landscape by holding one gradient
 82 constant while gradually shifting the other gradient along the
 83 x-axis, such that the decoupling environment pushes local
 84 fitness peaks toward novel regions of two-dimensional trait
 85 space (Fig. 1). We run 100 pairs of climate change simula-
 86 tions and null (stable-climate) simulations for each of eighteen
 87 scenarios resulting from the full factorial crossing of three key
 88 components of genomic architecture: genotypic redundancy,
 89 polygenicity, and linkage (Table 1).

90 We analyze variation in the resulting spatiotemporal pat-
 91 terns of gene flow, population size and density, and phenotypic
 92 distributions — all of which are emergent properties of our
 93 simulation parameterizations (Code Sample S1) — to test a
 94 series of hypotheses about the influence of genomic architec-
 95 ture on multivariate adaptation under climate change. First,
 96 we hypothesize that up-gradient gene flow will be higher under
 97 climate change than under a stable climate across all scenarios
 98 but that gene flow contributes least to climate change adap-
 99 tation when linkage is low and polygenicity is high. This is
 100 because we expect gene flow to always have at least some adap-
 101 tive value, but we also expect low-linkage, high-polygenicity
 102 architectures (i.e., 'dispersed' architectures (24)) to exhibit
 103 quick *in situ* adaptation via shifting allelic covariance among
 104 many small-effect alleles, facilitating phenotypic shifts in the
 105 absence of up-gradient gene flow. Second, we hypothesize
 106 that stronger linkage and higher polygenicity will reduce a

physical landscape



fitness landscape

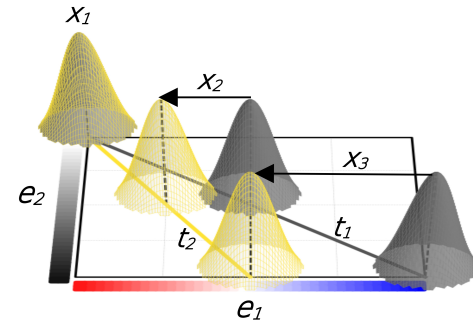


Fig. 1. Conceptual model of adaptation to climate change. The top panel depicts the two-layered physical landscape used in our simulations, showing the shifting environmental gradient (e_1) in a blue-red color ramp and the stable gradient (e_2) in a white-black color ramp. The landscape is shown both before climate change (t_1) and after (t_2). The bottom panel depicts a fitness landscape for two traits adapted to the shifting (e_1) and stable gradients (e_2). Three example positions on the physical landscape (x_1, x_2, x_3) are shown as boxes delineated y-axis cross-sections, both before climate change (gray) and after (yellow), and their corresponding fitness peaks are shown as color-matched kernels on the fitness landscape. The gray and yellow lines on the fitness landscape indicate the fitness optima defined by the environments that exist before (t_1) and after climate change (t_2). Shifts in local fitness peaks are shown as labeled arrows (x_2, x_3); the environment at the far left of the physical landscape does not change, so x_1 's fitness peaks are overlapping and have no shift.

107 population's adaptive capacity under climate change, manifesting
108 as greater reductions in population size and mean fitness
109 and more persistent maladaptation, because both conditions
110 impose longer expected wait times for the emergence of recom-
111 binant haplotypes that push phenotypes further from their
112 pre-change fitness peaks. Finally, we hypothesize that higher
113 genotypic redundancy will facilitate adaptation to shifting
114 gradients, much as it does on stable gradients (33, 35, 36),
115 resulting in smaller reductions in population size and mean
116 fitness.

117 Methods

118 **Simulations.** We performed simulations using Geonomics
119 (45), a Python (46) package for forward-time, agent-based,
120 continuous-space landscape genomic simulations. All of our
121 simulated scenarios feature a species with two traits, each of
122 which experiences selection on the basis of a different environ-
123 mental variable. Both environmental variables are modeled as
124 linear gradients running along the x-axis (Fig. 1) that initially
125 span environmental values from 1 to 0, left to right across the
126 landscape. The genome is modeled as an array of length L ,
127 which in our 2-trait simulations equals 2 times the number of
128 genes per trait. Instead of randomly assigning loci to either of
129 the two traits, we alternated locus trait assignment along the
130 genome to avoid creating islands of within-trait linkage that
131 would vary across iterations and introduce noise in our results.
132 The fitness of individuals is a function of the difference between
133 their local environmental values and their phenotypes, which
134 are determined by the additive effects of multiple loci (i.e.,
135 without pleiotropy or epistasis), a reasonable approximation of
136 many traits in real populations (32). Individuals have contin-
137 uous spatial coordinates, and their local environmental values
138 are found in the landscape cells within which their coordinates
139 fall. Each time step has a movement phase during which
140 each individual moves along a vector composed of a randomly
141 drawn direction (from a uniform circular distribution) and a
142 randomly drawn distance (from a $\text{Wald}(0.25, 0.5)$ distribution,
143 such that most movements are less than one landscape cell in
144 length).

145 Simulations start with a neutral burn-in period that does
146 not include differential fitness. The burn-in is concluded when
147 statistical tests of temporal and spatial population stability
148 are passed, at which point individuals are randomly assigned
149 genomes based on $0.5|0.5$ allele frequencies at all loci. Simula-
150 tions then run for 2,500 time steps with differential fitness,
151 generating a pattern of local adaptation to the initial environ-
152 ment. After that, one environmental layer undergoes a change
153 event in which the gradient's values shift over a period of 250
154 time steps, resulting in a final gradient that spans values from
155 1 to 0.5, left to right. This creates a scenario in which the
156 two environmental variables become decoupled, leading to the
157 emergence of novel environments (i.e. sites occupying new
158 values in two-dimensional environmental space), effectively
159 modeling a common phenomenon under climate change (41–
160 43). This generates spatially heterogeneous rates of climate
161 change, ranging from no change at the leftmost edge to 0.002
162 units per timestep at the rightmost edge. We chose this sce-
163 nario because one with spatially homogeneous rates of change
164 would generate an artefact of range expansion whose genomic
165 signal could not reliably be disentangled from that of climate
166 change adaptation. Hence, the approach we chose here allows

167 us to isolate the evolutionary dynamics resulting from the
168 components of genomic architecture that define our scenarios
169 and hypotheses. The pre-climate change population sizes in
170 our simulations varied around 5,800–6,100 individuals, which
171 yields mean times to fixation of approximately 16,000–17,000
172 time steps (18, 45), roughly an order of magnitude larger than
173 the total simulation length. Thus, the effects of drift during
174 these simulations should be low given the relatively large
175 population sizes.

176 We used a custom Python script to set values for the pa-
177 rameters of interest in our simulations: the number of loci
178 underlying each trait (parameter `n_loci`), the recombination
179 rate between neighboring loci (parameter `recomb`), and the
180 level of genotypic redundancy (parameter `redund`). The val-
181 ues we assigned to these parameters are provided in Table
182 1, and a visual depiction of the difference between low- and
183 high-redundancy scenarios for all phenotypes is provided in
184 Fig. S1. We ran the simulations on the `savio3` partition of
185 UC Berkeley's Savio computing cluster (each node has 96 GB
186 RAM and 32, 2.1-GHz Skylake processors). For each scenario,
187 we ran a total of 100 iterations, featuring a 250 time-step
188 climate change period with natural selection (henceforth, the
189 'main' scenarios), and 100 iterations of a paired null scenario
190 without natural selection (henceforth, the 'null' scenarios).
191 We set all other Geonomics parameters to their default val-
192 ues. Some values of interest that might be explicit parameter
193 settings in other simulation programs are instead emergent
194 properties in Geonomics; for example, the population size
195 values we report emerge from the interaction of several explicit
196 parameters, including the raster of local carrying capacities,
197 the population intrinsic growth rate, the number of offspring
198 per reproduction event, and the death rates resulting from the
199 parameters controlling density-dependent mortality and natu-
200 ral selection. The complete set of Geonomics parameters and
201 the values we assigned to them across all models are provided
202 in Code Sample S1. The parameters we set correspond best
203 to a scenario of a moderately mobile species with occasional
204 longer-distance dispersal, overlapping generations, and repeat
205 reproduction of small numbers of offspring.

206 Using a combination of internal Geonomics functions and
207 custom Python code, we designed a set of data outputs from
208 each model run to visualize results and test hypotheses. We
209 saved tables of the locations and phenotypes for all individuals
210 at the beginning and end of the climate change period. We
211 also saved time series of population size, mean fitness, and the
212 mean phenotype of the trait adapted to the shifting gradient.
213 We gathered this data at every time step for the 250 time
214 steps immediately before the onset of climate change, 250 time
215 steps during the climate change period, and 250 time steps
216 after climate change completed (hereafter, the 'post-change
217 period').

218 We also saved data on the vector directions of gene flow
219 occurring during climate change by keeping data for two ran-
220 domly chosen loci underlying the trait adapted to the shifting
221 environmental gradient (with positive effect) for all of the
222 individuals remaining in the final time step. Capturing loci ex-
223 pected to facilitate adaptation to increasing environmental val-
224 ues allowed us to track up-gradient gene flow, and it provided
225 equal sample sizes across scenarios for downstream analysis
226 (which was constrained to the number of positive-effect loci in
227 the low-polygenicity, low-redundancy scenarios). We collected

228 these data using an internal function that extracts data from
 229 the spatial pedigrees stored in the simulation's `tskit` (47)
 230 data structures. We also calculated a single summary metric
 231 of 'up-gradient gene flow' for each iteration:

$$232 GF_{up} = \frac{\sum_i^n \cos \theta}{n}, \cos \theta \geq 0,$$

233 where θ is the angle of gene flow, expressed counterclockwise
 234 from the right. The $\cos \theta \geq 0$ condition allowed us to track
 235 only rightward (up-gradient) gene flow and to omit leftward
 236 (down-gradient) gene flow which would be maladaptive for the
 237 positive-effect loci we tracked and, thus, low irrespective of
 238 scenario.

239 **Analysis.** We analyzed the results of our simulations using
 240 custom scripts written in Python (46) and R (48). To test
 241 our first hypothesis — that up-gradient gene flow should be
 242 greater under climate change scenarios — we first produced
 243 a visualization of the directional distributions of gene flow
 244 under all 18 scenarios, comparing between main and null
 245 simulations (Fig. 2) based on the random sample of the gene
 246 flow that occurred during the climate change period that we
 247 captured from our simulations. We then fitted a mixture of
 248 4 von Mises distributions to that data using the R package
 249 `mvnMF` (49), yielding 12 parameter estimates defining each
 250 simulation's fitted mixture distribution. For each of the 18
 251 scenarios, we then plotted the probability density function
 252 described by the means of all vectors of fitted parameters. We
 253 did this separately for null scenarios and for main scenarios
 254 then overlaid the results for the main scenarios (in red) on top
 255 of the null results (in blue; Fig. 2), providing a visualization
 256 of the directionality of gene flow within each climate change
 257 scenario compared to its null expectation.

258 We also ran a simple linear regression of the main vs. null
 259 difference in up-gradient gene flow density as a function of
 260 polygenicity, linkage, and redundancy. We coded the genomic
 261 architecture components as integer variables representing the
 262 levels of the parameter values used in the simulations (redundancy:
 263 low = 1, high = 2; polygenicity: low = 0, moderate = 1,
 264 high = 2; linkage: low = 0, moderate = 1, high = 2). We used
 265 the regression results to test both predictions for our first hy-
 266 pothesis: (1) that the main main - null difference in up-gradient
 267 gene flow should have 95% confidence intervals > 0 under all
 268 scenarios (calculated using the `stats` package's `predict.lm`
 269 function with the argument `interval = 'confidence'`), in-
 270 dicating significant up-gradient gene flow under climate change;
 271 and (2) that the coefficients for the linkage (β_l) and polygenicity
 272 (β_p) terms of the model should be significantly positive and
 273 negative, respectively, indicating that higher levels of gene flow
 274 are associated with stronger linkage and lower polygenicity.

275 To visually assess our second and third hypotheses, we
 276 created a series of plots comparing climate change-driven
 277 demographic shifts and maladaptation across all 18 scenarios
 278 and between our null and main models. First, we plotted
 279 the null and main time series of two demographic metrics,
 280 mean fitness and population size, for each of our 18 scenarios,
 281 combining the results for all 100 iterations under each scenario.
 282 For each time series we calculated the mean and 5th and
 283 95th percentiles at each time step (Figs. 3 and S2). We also
 284 summarized all scenarios in a pair of box plots (Fig. S2).

285 To better understand changes in population size and dis-
 286 tribution, we also mapped before and after comparisons of

287 population densities for all 18 main scenarios (Fig. S3). Each
 288 population density map was calculated as the mean population
 289 density at each cell on the landscape, averaged across all 100
 290 iterations.

291 Finally, to visualize maladaptation, we plotted each sce-
 292 nario's mean phenotypic distributions before and after climate
 293 change as scatter plots of the density of individuals occur-
 294 ring across two-dimensional trait space. We plotted lines and
 295 wedges depicting the average maladaptation observed across
 296 each scenario's 100 iterations (Fig. 4). We refer to the wedge
 297 as 'persistent maladaptation,' and we calculated it as the
 298 difference between: a) the area within two-dimensional trait
 299 space that the population's phenotypic distribution would
 300 have needed to shift through during the climate change event
 301 to remain optimally fit to its environment, and b) the observed
 302 area of phenotypic shift within a scenario's 100 simulations.
 303 We qualify this metric as 'persistent' to emphasize that it does
 304 not reflect transient maladaptation that arises but then resides
 305 during the period of climate change but rather reflects only
 306 maladaptation that remained at the end of the climate change
 307 period. To measure this area, we first determined the trian-
 308 gular area between the expected central tendency lines of the
 309 optimal two-dimensional phenotypic distributions before and
 310 after the climate change event. Then, for each model run, we
 311 used ordinary least squares (OLS) to fit a central tendency line
 312 to the 100-iteration ensemble phenotypic distribution observed
 313 at the end of the climate change event (fixing the y-intercept
 314 at the (1,1) point in phenotypic space, which represents the
 315 unchanging phenotypic optimum at the leftmost extent of
 316 the landscape). The area of the wedge between the expected
 317 and observed post-change central tendency lines provides our
 318 measure of a scenario's persistent maladaptation. We plotted
 319 before and after scatter plots of the ensemble datasets of in-
 320 dividuals' two-dimensional phenotypes (binned to a grid of
 321 regular points for interpretability). We also produced these
 322 plots (Fig. S4) using data from our null simulations to demon-
 323 strate that all differences in maladaptation observed between
 324 scenarios were attributable to climate change.

325 To statistically evaluate our results, we ran simple linear
 326 regressions for each of our three response variables measuring
 327 population-level changes during the climate change event —
 328 change in mean fitness, change in population size, and per-
 329 sistent maladaptation — with polygenicity, linkage, redundancy,
 330 and nullness serving as explanatory variables. We modeled
 331 nullness as a binary categorical variable (null = 0, main = 1)
 332 and again modeled the genomic architecture components as
 333 integer variables, as described above. We used these regres-
 334 sions to test our second (polygenicity and linkage) and third
 335 (redundancy) hypotheses. Specifically, our second hypothesis
 336 predicts that the coefficients of the linkage and polygenicity
 337 terms are significantly non-zero and negative (for changes
 338 in fitness-change and population size) and positive (for the
 339 maladaptation model), while our third hypothesis predicts sig-
 340 nificantly non-zero redundancy coefficients with the opposite
 341 signs.

342 Results

343 **Gene flow.** Under our simulations, climate change led to a
 344 nearly universal increase in up-gradient gene flow compared to
 345 null simulations with no change to either environmental vari-
 346 able. For all 18 of our simulated scenarios (Fig. 2), the simula-

347 tions with climate change exhibited greater up-gradient gene
 348 flow than the null scenarios, and linear regressions modeling the
 349 effects of linkage, redundancy, and polygenicity on up-gradient
 350 gene flow found that the fitted 95% confidence intervals for
 351 up-gradient gene flow were > 0 for all but one scenario (the
 352 moderate-polygenicity, low-linkage, high-redundancy scenario;
 353 Table S1). However, the magnitude of this increase in gene
 354 flow was minimal under some scenarios. We found that the
 355 difference in up-gradient gene flow between climate change
 356 and null simulations was positively correlated with linkage
 357 ($\beta_l = 0.0129 \pm 0.0006, P < 1 \times 10^{-15}$) and inversely correlated
 358 with polygenicity ($\beta_p = -0.0142 \pm 0.0006, P < 1 \times 10^{-15}$), cor-
 359 roborating our first hypothesis. Correspondingly, and in line
 360 with expectations, down-gradient gene flow was universally
 361 suppressed under climate change (Fig. 2). Of the three com-
 362 ponents of genomic architecture that we tested, polygenicity
 363 had the most striking effect on the extent to which up-gradient
 364 gene flow contributed to adaptation; moderate and high poly-
 365 genicity scenarios generally had much lower up-gradient gene
 366 flow than did low-polygenicity scenarios, with low-redundancy,
 367 independent-linkage scenarios being the main exception (Fig.
 368 2). Moderate-polygenicity scenarios actually showed the lowest
 369 overall increase in up-gradient gene flow, though differences
 370 between moderate- and high-redundancy scenarios were minor.
 371

372 **Linkage and polygenicity.** As expected, our null simulations
 373 showed essentially no changes in mean fitness (Fig. 2) or
 374 population size (Fig. S2), aside from small modeling artefacts
 375 present in both the null and climate-change scenarios, and the
 376 phenotypic distributions for the populations in these sim-
 377 ulations were stable through time (Fig. S4). The results of our
 378 climate change simulations exhibited decreases in population
 379 size and mean fitness that are the expected results of increasing
 380 maladaptation (10). They also revealed environment-tracking
 381 phenotypic shifts (Fig. 4) in line with expectations (Fig. 1),
 382 though these shifts lagged behind environmental change to
 383 some extent, producing suboptimal mean fitness at the end of
 384 the climate change period. Across scenarios, the demographic
 385 responses to climate change, in terms of population size and
 386 fitness, increased with increasing linkage (change in fitness:
 387 $\beta_l = -0.0018 \pm 0.0001, P < 1 \times 10^{-15}$; change in population
 388 size: $\beta_l = -33.330 \pm 1.287, P < 1 \times 10^{-15}$). We also found
 389 greater maladaptation, defined as the area in two-dimensional
 390 trait space separating the central line of a population's post-
 391 change phenotypic distribution from the central line of the
 392 distribution that would optimally track the changing envi-
 393 ronment (Figs. 4 and S4), associated with increasing linkage
 394 (maladaptation: $\beta_l = 0.0038 \pm 0.0004, P < 1 \times 10^{-15}$).

395 The magnitude of demographic responses also showed a
 396 signal of overall increase with increasing polygenicity (change
 397 in fitness: $\beta_p = -0.0022 \pm 0.0001, P < 1 \times 10^{-15}$; change in
 398 population size: $\beta_p = -15.070 \pm 1.287, P < 1 \times 10^{-15}$; mal-
 399 adaptation: $\beta_p = 0.0097 \pm 0.0004, P < 1 \times 10^{-15}$), although
 400 the trend was non-monotonic and complex. Responses were
 401 smallest at moderate polygenicity, more pronounced at low
 402 polygenicity, and highest at high polygenicity and low redun-
 403 dancy (Figs. 3 and S2). In fact, under high polygenicity
 404 and low redundancy, populations declined so strongly that
 405 adaptive capacity was effectively outstripped, and the declines
 406 persisted throughout the climate change period, with little
 407 indication of evolutionary rescue (i.e., stabilization and re-

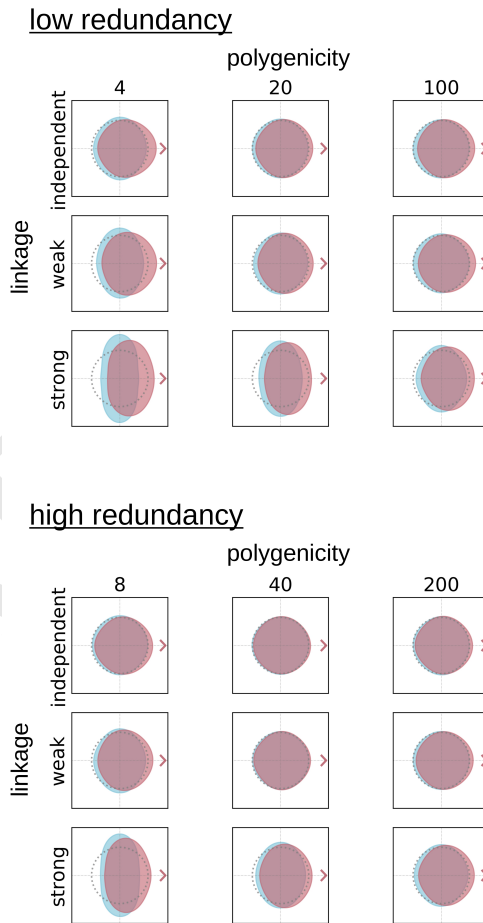
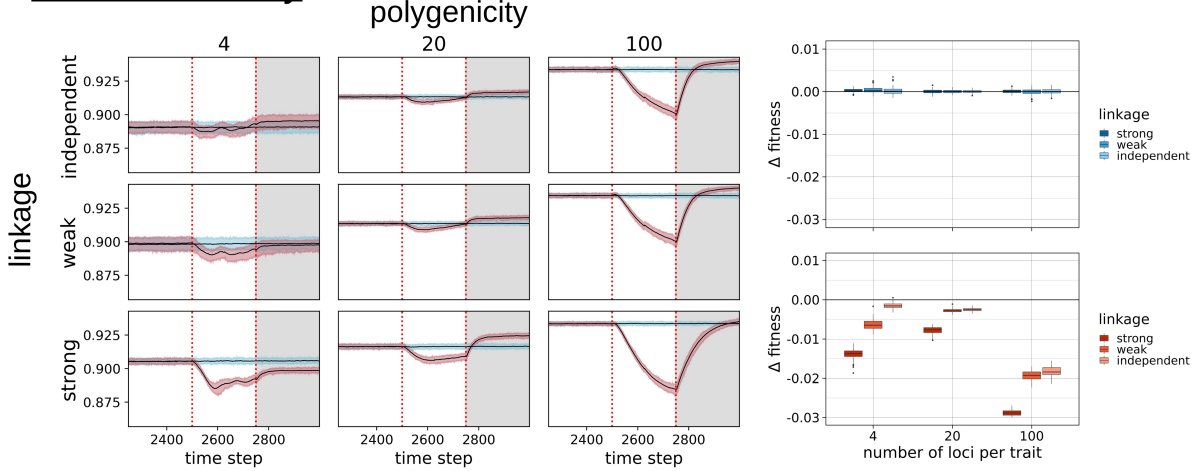


Fig. 2. Distributions of gene flow directions during the climate change period of our climate change simulations (red) compared to null simulations (blue) for our 18 scenarios. The shifting environmental gradient moves to the right (in the direction of the arrow) in our simulations, so rightward gene flow represents up-gradient gene flow, and upward and downward (i.e., 'on contour') gene flow is perpendicular to the environmental gradients. Down-gradient gene flow is expected to be maladaptive under all scenarios, explaining why it is universally suppressed relative to the null results (as evidenced by the blue distributional 'margins' extending to the left of the red distributions in all scenarios). There is a general trend toward increasing on-contour gene flow and decreasing up-gradient gene flow with decreasing linkage and increasing polygenicity.

low redundancy



high redundancy

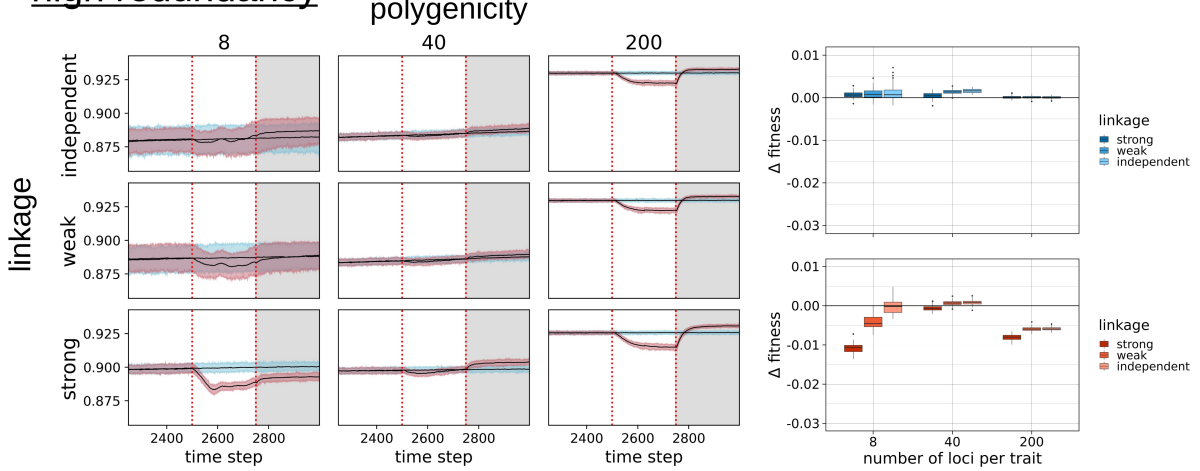


Fig. 3. Left: Mean fitness for all scenarios during the 250 time steps before, during, and after the climate change period (separated by red, dashed lines). Black lines represent the mean values, and the shaded red and blue areas represent variability envelopes (5th percentile to 95th percentile) for all replicates for climate change and null simulations, respectively. Right: Boxplots of changes in mean fitness during the climate change period for all scenarios. Null scenarios are plotted on the top in blue, and main scenarios are plotted on the bottom, in red. Within each plot, the scenarios are organized by polygenicity (number of loci per trait) on the x-axis and shaded by the strength of linkage.

408 bound) occurring until the post-change period (Figs. 3 and 4). The collapse of adaptive capacity in these scenarios is
 409 also visible in the large areas of phenotypic-shift shortfall in
 410 Fig. 4. The low-redundancy, high-polygenicity, strong-linkage
 411 scenario had such low adaptive capacity that mean fitness
 412 declined by 5.2% on average (from 0.934 to 0.885), mean pop-
 413 ulation size declined by 17.1% on average (from 6326 to 5246
 414 individuals), and the simulated population ceased to occupy
 415 the rightmost, fastest-changing portion of the landscape (Fig.
 416 4).

418 **Genotypic redundancy.** Our high-redundancy scenarios showed
 419 consistently smaller demographic responses to climate change,
 420 less-prominent up-gradient gene flow, and higher adaptive
 421 capacity, than their low-redundancy counterparts (change in
 422 fitness: $\beta_r = 0.0040 \pm 0.0002, P < 1 \times 10^{-15}$; change in pop-
 423 ulation size: $\beta_r = 39.060 \pm 2.101, P < 1 \times 10^{-15}$; maladaptation:
 424 $\beta_r = -0.0098 \pm 0.0006, P < 1 \times 10^{-15}$), consistent with our hy-
 425 pothesis that genotypic redundancy can facilitate adaptation

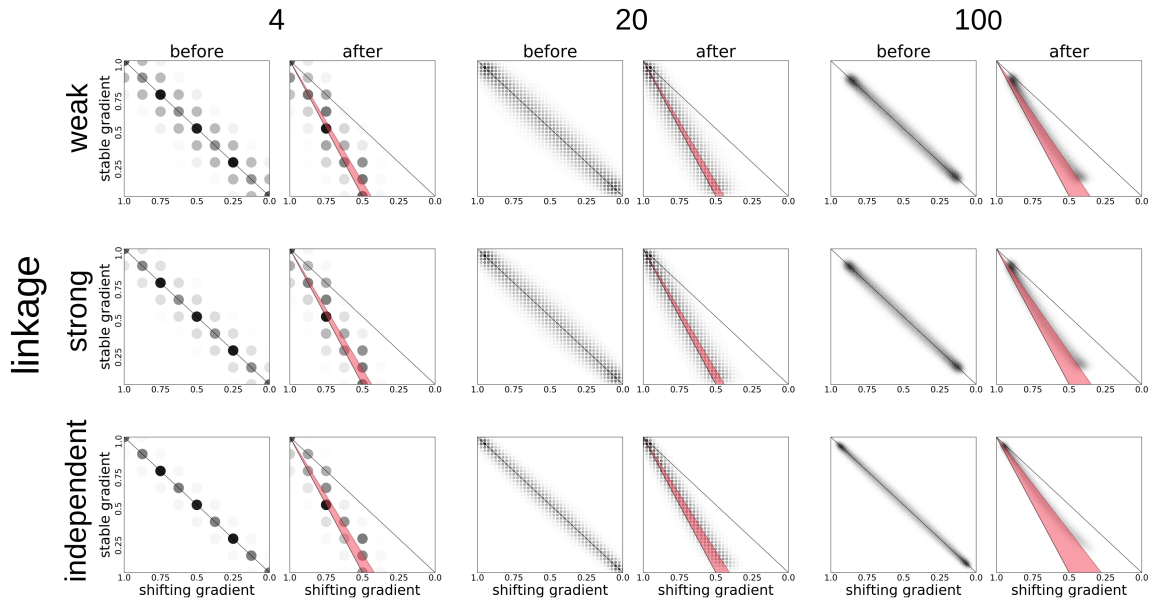
426 to shifting environmental gradients (Figs. 2 and S2). This
 427 effect was most pronounced in the high-polygenicity scenarios,
 428 which exhibited much milder demographic decline under high
 429 redundancy compared to low redundancy, despite still showing
 430 no evidence of demographic rebound until after climate change
 431 (Fig. 3). Indeed, increased redundancy put the demographic
 432 declines under these scenarios on par with those of the low
 433 polygenicity scenarios (Figs. 3 and S2).

Discussion

434 Current theoretical understanding of evolutionary responses
 435 to climate change largely derives from a simplified mechanistic
 436 model in which adaptation is universally facilitated by up-
 437 gradient gene flow. This model also serves as the inspiration
 438 for some climate-smart approaches to biodiversity manage-
 439 ment (e.g., assisted gene flow; (10)). However, adopting this
 440 model as the basis for theoretical and mechanistic research
 441 risks overlooking the influence of genomic architecture on mul-
 442 tivariate adaptation to environmental change. Starting from a
 443

low redundancy

polygenicity



high redundancy

polygenicity

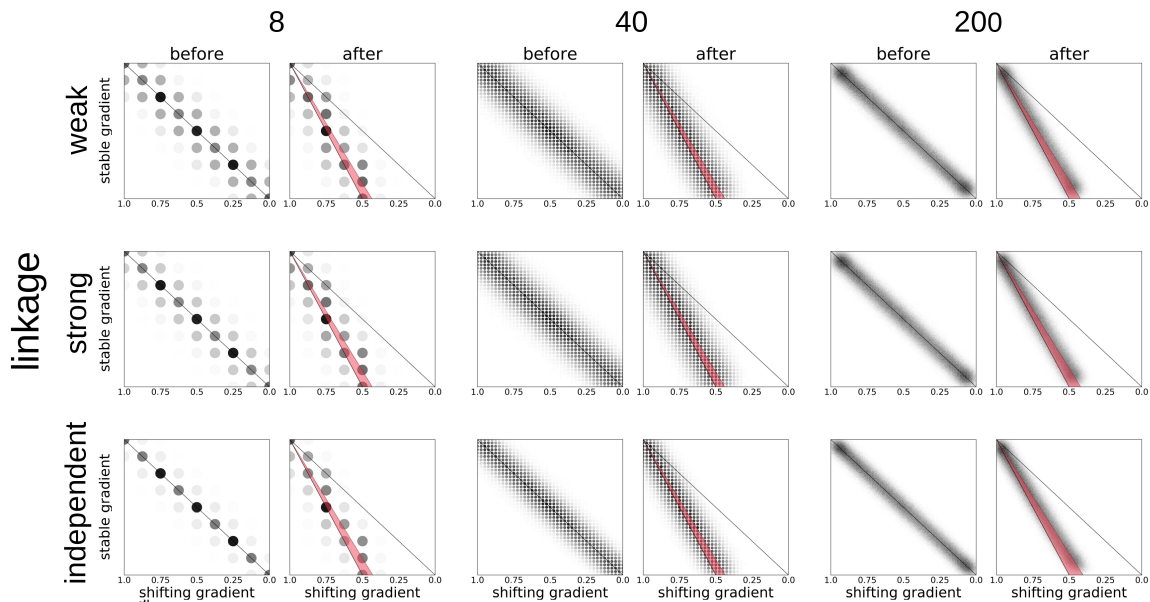


Fig. 4. Scatterplots of the observed versus expected phenotypic shift during the climate change period for all 18 of our simulated scenarios. For each scenario, the left ('before') scatterplot shows the distribution of phenotypes before climate change begins, and the right ('after') scatterplot shows how the distribution has shifted by the end of the climate change period. The trait adapted to the shifting environmental gradient is distributed along the x-axis, with the trait adapted to the stable gradient on the y-axis. Each plot is an ensemble of the results for all 100 replicates of each scenario. The size and opacity of each point represents the number of individuals exhibiting that two-dimensional phenotype. The gridded arrangement of the points in each scatterplot is a function of the number of loci per trait, which determines the set of possible phenotypes. Solid black lines delineate the shifts in the phenotypic distributions' central tendencies that are expected to take place during the climate change period, dotted black lines depict the observed distributions' central tendencies, and red wedges depict the differences between the expected and observed distributions ('phenotypic shortfall').

more realistic, multi-trait framework, our simulations demonstrate that up-gradient gene flow does indeed occur under climate change but that its contributions to local adaptation and persistence may be constrained by polygenicity, genotypic redundancy and, to a lesser extent, linkage. Given the range of plausible genomic architectures we simulate (6, 20, 29–32), these results raise the compelling possibility that up-gradient gene flow, while unlikely to be entirely maladaptive, could play a limited role in climate change adaptation in many systems. This may be especially true in systems where climate-adapted traits have more dispersed architectures — for example, architectures composed of many genes of small effect (24). This poses an important question for subsequent research: how often are the genomic architectures underlying climate-adapted traits dispersed versus concentrated?

We also show that the genomic architecture of climate-adapted traits can influence the nature and size of demographic responses to climate change. Our results suggest that strong linkage between non-neutral loci, especially under high polygenicity, can increase maladaptation and demographic decline during climate change. In the most extreme case, evolutionary rescue was absent; high polygenicity and low redundancy combined to drive dramatic and persistent demographic declines and even caused local extinction when linkage was strong. This was unexpected in light of previous work reporting that dispersed architectures produce stable, resilient phenotypic clines despite transient genotypic composition (24, 33) and, thus, that species with such architectures could exhibit rapid local adaptation (50). We did, nonetheless, expect evolutionary responses to climate change to be slower in these scenarios, because natural selection is less effective on smaller-effect alleles, gene flow may have more of a swamping effect for these alleles, and high linkage leads to longer expected wait times for the generation of novel, adaptive recombinant genotypes. We did not, however, expect adaptive capacity to be completely outstripped. Yet, it appears that the rate of environmental change simply exceeded the pace of adaptation. This is evidenced by the quick demographic rebound that occurred in the ‘post-change’ periods (Fig. 3). This rebound was likely driven by the same evolutionary dynamics that occur during evolutionary rescue, but in these extreme scenarios it only emerged once environmental change had ceased.

Remarkably, we also observed higher maladaptation and larger demographic declines in our low-polygenicity scenarios with fewer, larger-effect alleles. Demographic decline was least pronounced in our moderate-polygenicity models. This contrasts with previous work finding that adaptation to a gradient is more effective under either concentrated or dispersed genomic architectures (25). This disagreement may be attributable to the difference in timeframes between adaptation to a univariate environmental gradient and adaptation to a decoupled, multivariate gradient. Adaptation to a single, static gradient can proceed gradually, which may favor large-effect alleles or allele-clusters over longer time scales, once they have arisen by mutation, recombination, gene flow, or a combination thereof (24, 33). Longer term, gradual change scenarios may also favor dispersed architectures in temporally fluctuating environments (24, 25, 51, 52). However, the sudden onset of persistent environmental change in a population that is already locally adapted triggers a ‘race against time,’ and genomic architectures with optimal adaptive capacity may

be the ‘middle ground’ architectures that comprise freely recombining loci with small enough effect sizes to avoid large declines in fitness from migration load but with large enough effect sizes to allow for effective natural selection and to avoid the long wait times necessary for recombination to cluster many adaptive loci into larger-effect haplotypes. This presents the surprising possibility that an ‘evolutionary trade-off’ may exist, such that mid-effect-size alleles may confer maximal adaptive capacity to environmental change.

The fact that high genotypic redundancy reduces demographic decline, across all scenarios, contributes to the growing recognition of the importance of redundancy as a driver of evolutionary outcomes for polygenic traits (24, 34). This also presents a possible mechanism to be explored in real-world populations living at colder range edges. Much like the local populations in the rightmost region of our low-redundancy scenarios, these local populations could already be at the edge of the phenotypic space defined by their standing genetic variation. In this case, segregating redundancy (34) and, thus, adaptive capacity would be low, so vulnerability to local extinction would be substantial. However, species whose cold range edges are predominantly determined by geographic barriers or biotic interactions rather than climate limits (53) could feature local populations more similar to our high-redundancy scenarios; segregating redundancy would be higher, so selection would be balancing rather than directional, and adaptive capacity would be substantial. Hence, *in situ* adaptation would be a substantial contributor to adaptive capacity in these scenarios — an implication supported by the fact that we observed reduced up-gradient gene flow across all high-redundancy scenarios.

Our findings also contribute new insight to the theoretical understanding of local adaptation with recombination. Recombination is generally regarded as disadvantageous in situations of clinal adaptation with gene flow, because it disrupts the association between adaptive loci underlying a single trait (12). Unstable environments experiencing stochastic temporal fluctuations are considered a major exception (12), but our results suggest that this may also extend to environments undergoing monotonic change such as that caused by climate change. In fact, recombination may be advantageous under these conditions, particularly when species have distinct traits simultaneously adapted to decoupled environmental gradients. This advantage likely arises because recombination allows for more effective *in situ* adaptation by shifting allelic covariance, despite still disrupting the associations between loci that would otherwise allow for the development of larger-effect gene clusters. This suggests that *in situ* shifts in allelic covariance provide an alternative to adaptive gene flow as a mechanism for evolutionary rescue, especially in multi-trait systems where gene flow can be adaptive for shifting climatic gradients but maladaptive with respect to other, decoupled gradients.

A major challenge in simulation-based research is the complexity of the high-dimensional parameter space that could be explored. Useful and informative studies can be constructed by focusing on a small set of key parameters while holding others at reasonable values, as we have done here. This nonetheless leaves unexplored a number of secondary parameters that can have non-negligible influence over the complex ecological phenomena of interest. In the case of evolutionary responses to climate change this provides various areas for future research.

These include population size, a major determinant of the relative strengths of drift and natural selection (54) and of the wait time to emergence of recombinant haplotypes (55); movement behavior, a key factor influencing migration-selection dynamics (17, 18, 21); allelic effect size distributions (56), which are omitted here in favor of a single, fixed effect size; and the spatiotemporal structure of the environment, including gradient geometries, slopes, orientations, and rates of change (57). Additionally, important and conservation-relevant insight could emerge from the integration of other dimensions of climate change ecology, including range shifts (58), plasticity (1), and range-wide variation in population densities (10). Finally, more complex evolutionary scenarios could also be explored, including pleiotropy and epistasis (59), hybridization (60), life history variation, and even multiple traits that differ in the complexity of their genomic architectures — a realistic scenario that could exhibit different evolutionary outcomes than the ones we describe here.

Conclusions

Adaptive gene flow and *in situ* adaptation are two of the main processes by which species may persist under climate change. Evaluating the conditions under which they are likely to contribute to species persistence is essential for better understanding microevolutionary responses to climate change and for informing management efforts. Our simulations show that genomic architecture can play an important, but largely overlooked, role in driving evolutionary outcomes. This includes determining the relative effectiveness of these two processes, the magnitude and persistence of maladaptation, and the likelihood of concomitant demographic decline or evolutionary rescue. These findings highlight the importance of considering multivariate environmental gradients for climate change research, and suggest that the genomic architecture underlying traits adapted to those gradients has direct consequences for how species respond to environmental change.

ACKNOWLEDGMENTS. We thank A. P. Bishop, T. Dawson, J. Frederick, N. Graham, M. Kelly, M. McElroy, E. Westeen, G. Wogan, and M. Yuan for feedback and guidance on various iterations of the simulations presented herein. We thank Berkeley Research Computing for providing access to the Savio computing cluster. We thank D. Ehrenfeld, N. Fefferman, M. Fitzpatrick, and L. Plough for cultivating an interest in conservation genetics. Lastly, we thank M. Terasaki Hart, C. Nemec-Hart, G. Hart, J. Hart, and M. Tylka for supporting and encouraging a lifetime of curiosity about nature, and C. Adjuah, B. Evans, R. Pérez Joglar, Y. Y. Ma, and J. Redman for the great company during long periods of solitude. This work was supported by a Berkeley Fellowship from University of California, Berkeley (to D.E.T.H.), by a Bezos Earth Fund grant to The Nature Conservancy (which covered some time for D.E.T.H.), and by National Science Foundation grant DEB1845682 (to I.J.W.).

1. Luis-Miguel Chevin, Russell Lande, and Georgina M. Mace. Adaptation, Plasticity, and Extinction in a Changing Environment: Towards a Predictive Theory. *PLoS Biology*, 8(4):e1000357, 2010. ISSN 1544-9173. .
2. Katherine A. Harrison, Alexandra Pavlova, Marina Telonis-Scott, and Paul Sunnucks. Using genomics to characterize evolutionary potential for conservation of wild populations. *Evolutionary Applications*, 7(9):1008–1025, 2014. ISSN 1752-4571. .
3. Adrienne B. Nicotra, Erik A. Beever, Amanda L. Robertson, Gretchen E. Hofmann, and John O’Leary. Assessing the components of adaptive capacity to improve conservation and management efforts under global change. *Conservation Biology*, 29(5):1268–1278, 2015. ISSN 1523-1739. .
4. Ana Vilas, Andrés Pérez-Figueroa, Humberto Quesada, and Armando Caballero. Allelic diversity for neutral markers retains a higher adaptive potential for quantitative traits than expected heterozygosity. *Molecular Ecology*, 24(17):4419–4432, 2015. ISSN 1365-294X. .
5. Alisa A. Wade, Brian K. Hand, Ryan P. Kovach, Gordon Luikart, Diane C. Whited, and Clint C. Muhlfeld. Accounting for adaptive capacity and uncertainty in assessments of species’ climate-change vulnerability. *Conservation Biology*, 31(1):136–149, 2017. ISSN 0888-8892. .

6. Kirsten Bomblies and Catherine L Peichel. Genetics of adaptation. *Proceedings of the National Academy of Sciences*, 119(30):e2122152119, 2022. 632
633
7. Scott R. Loarie, Philip B. Duffy, Healy Hamilton, Gregory P. Asner, Christopher B. Field, and David D. Ackerly. The velocity of climate change. *Nature*, 462(7276):1052–1055, 2009. ISSN 0028-0836. . 634
635
636
8. D. D. Ackerly, S. R. Loarie, W. K. Cornwell, S. B. Weiss, H. Hamilton, R. Branciforte, and N. J. B. Kraft. The geography of climate change: implications for conservation biogeography. *Diversity and Distributions*, 16(3):476–487, 2010. ISSN 1472-4642. . 637
638
639
9. Joe Bellis, David Bourke, Joyce Maschinski, Katie Heineman, and Sarah Dalrymple. Climate suitability as a predictor of conservation translocation failure. *Conservation Biology*, 34(6):cobi.13518, 2020. ISSN 0888-8892. . URL <https://onlinelibrary.wiley.com/doi/abs/10.1111/cobi.13518>. 640
641
642
643
10. Sally N. Aitken and Michael C. Whitlock. Assisted Gene Flow to Facilitate Local Adaptation to Climate Change. *Annual Review of Ecology, Evolution, and Systematics*, 44(1):367–388, 2013. ISSN 1543-592X. . 644
645
646
11. Montgomery Slatkin. Gene flow and the geographic structure of natural populations. *Science*, 236(4803):787–792, 1987. 647
648
12. Anna Tigano and Vicki L Friesen. Genomics of local adaptation with gene flow. *Molecular ecology*, 25(10):2144–2164, 2016. 649
650
13. Jeffrey L Feder, Richard Gejji, Sam Yeaman, and Patrik Nosil. Establishment of new mutations under divergence and genome hitchhiking. *Philosophical Transactions of the Royal Society B: Biological Sciences*, 367(1587):461–474, 2012. 651
652
653
14. Graham Bell and Andrew Gonzalez. Adaptation and evolutionary rescue in metapopulations experiencing environmental deterioration. *Science*, 332(6035):1327–1330, 2011. 654
655
15. Ian J. Wang and Gideon S. Bradburd. Isolation by environment. *Molecular Ecology*, 23(23):5649–5662, 2014. ISSN 1365-294X. . 656
657
16. Thomas Lenormand. Gene flow and the limits to natural selection. *Trends in Ecology & Evolution*, 17(4):183–189, 2002. ISSN 0169-5347. . 658
659
17. John Burdon Sanderson Haldane. A mathematical theory of natural and artificial selection.(part vi, isolation.). In *Mathematical proceedings of the Cambridge philosophical society*, volume 26.2, pages 220–230. Cambridge University Press, 1930. 660
661
662
18. Sewall Wright. Evolution in Mendelian populations. *Genetics*, 16:97–159, 1931. 663
19. Joseph Felsenstein. The theoretical population genetics of variable selection and migration. *Annual review of genetics*, 10(1):253–280, 1976. 664
665
20. Neda Barghi, Joachim Hermisson, and Christian Schlöterer. Polygenic adaptation: a unifying framework to understand positive selection. *Nature Reviews Genetics*, 21(12):769–781, 2020. 666
667
668
21. N. H. Barton. Clines in polygenic traits. *Genetics Research*, 74(3):223–236, 1999. ISSN 1469-5073. . 669
670
22. Jonathan K Pritchard, Joseph K Pickrell, and Graham Coop. The genetics of human adaptation: hard sweeps, soft sweeps, and polygenic adaptation. *Current biology*, 20(4):R208–R215, 2010. 671
672
673
23. Jonathan K Pritchard and Anna Di Rienzo. Adaptation—not by sweeps alone. *Nature Reviews Genetics*, 11(10):665–667, 2010. 674
675
24. Sam Yeaman. Evolution of polygenic traits under global vs local adaptation. *Genetics*, 220(1), 2022. . 676
677
25. Sam Yeaman and Michael C. Whitlock. The genetic architecture of adaptation under migration-selection balance. *Evolution*, 65(7):1897–1911, 2011. ISSN 1558-5646. . 678
679
26. Valérie Le Corre and Antoine Kremer. The genetic differentiation at quantitative trait loci under local adaptation. *Molecular ecology*, 21(7):1548–1566, 2012. 680
681
27. Arnaud Martin and Virginie Orgogozo. The loci of repeated evolution: a catalog of genetic hotspots of phenotypic variation. *Evolution*, 67(5):1235–1250, 2013. 682
683
28. Jasmin S Rees, Sergi Castellano, and Aida M Andrés. The genomics of human local adaptation. *Trends in Genetics*, 36(6):415–428, 2020. 684
685
29. Evan A. Boyle, Yang I. Li, and Jonathan K. Pritchard. An Expanded View of Complex Traits: From Polygenic to Omnipgenic. *Cell*, 169(7):1177–1186, 2017. ISSN 0092-8674. . 686
687
30. Matthew V Rockman. The qtp program and the alleles that matter for evolution: all that’s gold does not glitter. *Evolution: International Journal of Organic Evolution*, 66(1):1–17, 2012. 688
689
31. Outi Savolainen, Martin Lascoux, and Juha Merilä. Ecological genomics of local adaptation. *Nature Reviews Genetics*, 14(11):807–820, 2013. 690
691
32. Guy Sella and Nicholas H Barton. Thinking about the evolution of complex traits in the era of genome-wide association studies. *Annual review of genomics and human genetics*, 20:461–493, 2019. 692
693
694
33. Sam Yeaman. Local adaptation by alleles of small effect. *The American Naturalist*, 186(S1):S74–S89, 2015. 695
696
34. Áki J Láruson, Sam Yeaman, and Katie E Lotterhos. The importance of genetic redundancy in evolution. *Trends in Ecology & Evolution*, 35(9):809–822, 2020. 697
698
35. Neda Barghi, Raymond Tobler, Viola Nolte, Ana Marija Jakšić, François Mallard, Kathrin Anna Otte, Marlies Dolezal, Thomas Taus, Robert Kofler, and Christian Schlöterer. Genetic redundancy fuels polygenic adaptation in *Drosophila*. *PLoS Biology*, 17(2):e3000128, 2019-2. ISSN 1544-9173. . 699
700
701
702
36. Marie Manceau, Vera S Domingues, Catherine R Linnen, Erica Bree Rosenblum, and Hopi E Hoekstra. Convergence in pigmentation at multiple levels: mutations, genes and function. *Philosophical Transactions of the Royal Society B: Biological Sciences*, 365(1552):2439–2450, 2010. 703
704
705
706
37. Katja Schifflers, Elizabeth C. Bourne, Sébastien Lavergne, Wilfried Thuiller, and Justin M. J. Travis. Limited evolutionary rescue of locally adapted populations facing climate change. *Philosophical Transactions of the Royal Society B: Biological Sciences*, 368(1610):20120083, 2013. ISSN 0962-8436. . 707
708
709
710
38. Frédéric Guillaume. Migration-induced phenotypic divergence: the migration–selection balance of correlated traits. *Evolution: International Journal of Organic Evolution*, 65(6):1723–1738, 2011. 711
712
713
39. Shawn M. Crimmins, Solomon Z. Dobrowski, Jonathan A. Greenberg, John T. Abatzoglou, and Alison R. Mynsberge. Changes in Climatic Water Balance Drive Downhill Shifts in Plant 714
715

716 Species' Optimum Elevations. *Science*, 331(6015):324–327, 2011. ISSN 0036-8075. .

717 40. Christopher Daly, David R. Conklin, and Michael H. Unsworth. Local atmospheric decoupling
718 in complex topography alters climate change impacts. *International Journal of Climatology*, 30
719 (12):1857–1864, 2010. ISSN 1097-0088. .

720 41. John W. Williams and Stephen T. Jackson. Novel climates, no-analog communities, and
721 ecological surprises. *Frontiers in Ecology and the Environment*, 5(9):475–482, 2007. ISSN
722 1540-9309. .

723 42. John W. Williams, Stephen T. Jackson, and John E. Kutzbach. Projected distributions of novel
724 and disappearing climates by 2100 AD. *Proceedings of the National Academy of Sciences*,
725 104(14):5738–5742, 2007. ISSN 0027-8424. .

726 43. Matthew C. Fitzpatrick, Jessica L. Blois, John W. Williams, Diego Nieto-Lugilde, Kaitlin C.
727 Maguire, and David J. Lorenz. How will climate novelty influence ecological forecasts? using
728 the quaternary to assess future reliability. *Global Change Biology*, 24(8):3575–3586, 2018.
729 ISSN 1354-1013. .

730 44. Thibaut Capblancq, Matthew C. Fitzpatrick, Rachael A. Bay, Moises Exposito-Alonso, and
731 Stephen R. Keller. Genomic Prediction of (Mal)Adaptation Across Current and Future Climatic
732 Landscapes. *Annual Review of Ecology, Evolution, and Systematics*, 51(1):1–25, 2020. ISSN
733 1543-592X. .

734 45. Drew E Terasaki Hart, Anusha P Bishop, and Ian J Wang. Geonomics: forward-time, spatially
735 explicit, and arbitrarily complex landscape genomic simulations. *Molecular Biology and
736 Evolution*, pages msab175–, 2021. ISSN 0737-4038. .

737 46. Guido Van Rossum and Fred L Drake Jr. *Python reference manual*. Centrum voor Wiskunde
738 en Informatica Amsterdam, 1995.

739 47. Jerome Kelleher, Kevin R. Thornton, Jaime Ashander, and Peter L. Ralph. Efficient pedigree
740 recording for fast population genetics simulation. *PLOS Computational Biology*, 14(11):
741 e1006581, 2018. ISSN 1553-7358. . URL <http://dx.plos.org/10.1371/journal.pcbi.1006581>
742 <https://journals.plos.org/ploscompbiol/article?id=10.1371/journal.pcbi.1006581>.

743 48. R Core Team. *R: A Language and Environment for Statistical Computing*. R Foundation for
744 Statistical Computing, Vienna, Austria, 2021. URL <https://www.R-project.org/>.

745 49. Kurt Hornik and Bettina Grüün. movMF: An R package for fitting mixtures of von mises-fisher
746 distributions. *Journal of Statistical Software*, 58(10):1–31, 2014. .

747 50. Sally N Aitken, Sam Yeaman, Jason A Holliday, Tongli Wang, and Sierra Curtis-McLane. Adap-
748 tation, migration or extirpation: climate change outcomes for tree populations. *Evolutionary
749 applications*, 1(1):95–111, 2008.

750 51. Reinhart Bürger and Alexander Gimelfarb. Fluctuating environments and the role of mutation
751 in maintaining quantitative genetic variation. *Genetics Research*, 80(1):31–46, 2002.

752 52. Alexey S Kondrashov and Lev Yu Yampolsky. High genetic variability under the balance
753 between symmetric mutation and fluctuating stabilizing selection. *Genetics Research*, 68(2):
754 157–164, 1996.

755 53. Chris D Thomas. Climate, climate change and range boundaries. *Diversity and Distributions*,
756 16(3):488–495, 2010.

757 54. Gemma GR Murray, André ER Soares, Ben J Novak, Nathan K Schaefer, James A Cahill,
758 Allan J Baker, John F Demboski, Andrew Doll, Rute R Da Fonseca, Tara L Fulton, et al. Natural
759 selection shaped the rise and fall of passenger pigeon genomic diversity. *Science*,
760 358(6365):951–954, 2017.

761 55. Freddy B Christiansen, Sarah P Otto, Aviv Bergman, and Marcus W Feldman. Waiting with
762 and without recombination: the time to production of a double mutant. *Theoretical population
763 biology*, 53(3):199–215, 1998.

764 56. H Allen Orr. The population genetics of adaptation: the distribution of factors fixed during
765 adaptive evolution. *Evolution*, 52(4):935–949, 1998.

766 57. Kylla M. Benes and Matthew E.S. Bracken. Interactive effects of large- and local-scale
767 environment gradients on phenotypic differentiation. *Ecology*, 101(8):e03078, 2020. ISSN
768 0012-9658. . URL <https://esajournals.onlinelibrary.wiley.com/doi/abs/10.1002/ecy.3078>?af=R
769 <https://onlinelibrary.wiley.com/doi/abs/10.1002/ecy.3078>.

770 58. Christopher Weiss-Lehman and Allison K Shaw. Spatial Population Structure Determines
771 Extinction Risk in Climate-Induced Range Shifts. *The American naturalist*, 195(1):31–42,
772 2020-1. ISSN 1537-5323. . URL <http://www.ncbi.nlm.nih.gov/pubmed/31868544>.

773 59. Ken A. Thompson. Experimental Hybridization Studies Suggest That Pleiotropic
774 Alleles Commonly Underlie Adaptive Divergence between Natural Populations.
775 <https://doi.org/10.1086/708722>, 196(1):000–000, 2020. ISSN 0003-0147. . URL
776 <https://www.journals.uchicago.edu/doi/10.1086/708722>?ai=sa&mi=0&af=R
777 <https://www.journals.uchicago.edu/doi/10.1086/708722>?ai=sa&mi=0&af=R.

778 60. Sheela P Turbek and Scott A Taylor. Hybridization provides climate resilience. *Nature Climate
779 Change*, pages 1–2, 2023.